JMEPEG (2018) 27:2388–2393
https://doi.org/10.1007/s11665-018-3317-7

1059-9495/$19.00

Effect of Hot Rolling on the Microstructure and Mechanical Properties of Nitrogen Alloyed Austenitic Stainless Steel

S. Chenna Krishna, N.K. Karthick, Abhay K. Jha, Bhanu Pant, and Roy M. Cherian

(Submitted April 14, 2017; in revised form January 31, 2018; published online April 2, 2018)

In the present investigation, the effect of multi-pass hot rolling in the temperature range of 700–1000 °C on the microstructure and mechanical properties of nitrogen alloyed austenitic stainless steel was studied with the aid of optical microscopy, tensile testing and x-ray diffraction measurements. The microstructural changes that occurred in the hot rolled specimens were elongation of grains in rolling direction, nucleation of new grains at the grain boundaries of elongated grains and growth of nucleated grains to form fully recrystallized grains. Elongated grains formed at lower rolling temperature (700–800 °C) due to inadequate strain/temperature for the initiation of dynamic recrystallization. At higher rolling temperature (900–1000 °C), fine grains formed due to dynamic recrystallization. Tensile properties showed strong dependency on the rolling temperature. Tensile strength increased with the decrease in the rolling temperature at the cost of ductility. Maximum strength was observed in samples hot rolled at 700 °C with yield strength of 917 MPa and ductility of 25%. This variation in the tensile properties with the rolling temperature is attributed to changes in the dislocation density and grain structure. The estimated yield strength from the dislocation density, solid solution and grain boundary strengthening closely matched with experimentally determined yield strength confirming the role of dislocation density and grain size in the strengthening.

Keywords hot rolling, nitrogen-alloyed austenitic stainless steel, strengthening

1. Introduction

Nitrogen alloyed austenitic stainless steels (ASS) are important class of stainless steels because of the lower cost and improved properties compared to classical ASS (Ref 1, 2). Nitrogen is a strong solid solution strengthener and austenite stabilizer. In addition, nitrogen has certain advantages compared to carbon: (i) Nitrogen reduces the tendency of austenite-to-martensite transformation due to deformation or cryo-treatment and formation of ferrite (Ref 3), (ii) higher solubility reduces the formation of precipitates at a given level of strengthening (Ref 1), (iii) it enhances grain boundary strengthening (Ref 2, 3) and (iv) improvement in impact toughness (Ref 4) and the pitting corrosion resistance (Ref 5, 6). The steel used in the present study has 0.2% nitrogen and does not respond to precipitation hardening. The main strengthening mechanisms are grain size strengthening, solid solution strengthening and dislocation strengthening. Therefore, improvement in the mechanical properties can be achieved by hot working, warm working, cold rolling and annealing (Ref 3, 4). Frechard et al. (Ref 5) studied the mechanical behavior of warm rolled nitrogen alloy ASS (Uranus B66) and reported improvement in mechanical properties at the cost of ductility. Dischin and Kenny reported that yield strength, hardness and grain size followed the Hall–Petch relationship for the range of grain size analyzed in SS304 and high nitrogen ASS (Fe-18.5Cr-1.07Cu-11.4Mn-0.37) (Ref 6). Kim studied the effect of grain refinement induced by nitrogen on high temperature mechanical properties in 316LN stainless steel and reported improvement in the tensile properties (Ref 7). The effect of cold rolling and annealing on the mechanical properties and microstructure of a high nitrogen austenitic stainless steel was studied by Bing et al. (Ref 4). There are limited systematic studies on the hot rolling of nitrogen alloyed austenitic stainless to improve the tensile strength. The purpose of the investigation was to study the effect of rolling temperature (700–1000 °C) on the microstructure and mechanical properties with an emphasis to achieve different combinations of strength and ductility.

S. Chenna Krishna, N.K. Karthick, Abhay K. Jha, Bhanu Pant, and **Roy M. Cherian**, Materials and Mechanical Entity, Vikram Sarabhai Space Centre, Trivandrum 695022, India. Contact e-mail: chenna.sk@gmail.com.

2. Material and Method

The chemical composition of the austenitic stainless steel used in the present study is given in Table 1. Annealed plates (AS) of 120 mm (length), 80 mm (width) and 10 mm (thickness) were used as input for hot rolling. Plates were preheated at a temperature (700–1000 °C) for 30 min before feeding into the rollers. Hot rolling was done using a rolling mill with 290 mm diameter rolls at a peripheral speed of 10 m min^{-1}. A total strain of 0.94 was induced by multi-pass rolling with a reduction of 15% in thickness per pass. The hot rolled plates after the final pass were air cooled, and thickness of the plates was 4.4 mm. The annealed and hot rolled specimens were characterized for mechanical properties and microstructure. The hot rolled samples will be referred as follows: hot rolled at 700 °C (HR700). Microstructural characterization of the specimens was performed by optical microscopy using bright-field

Table 1 Chemical composition of the nitrogen alloyed austenitic stainless steel (SS 202)

Element	Cr	Ni	Mn	C	N	Si	S	P	Fe
Weight%	18.2	5.1	6.9	0.06	0.21	0.2	0.005	0.013	Bal

and dark-field mode. Samples for metallography were prepared by mechanical polishing using emery paper, alumina and diamond paste. Duly polished samples were electrolytically etched with 10% oxalic acid (12 V, 12 s) and examined under an optical metallurgical microscope. Grain size was measured by linear intercept method using image analysis software (Imagej); 100 grains were measured to arrive at the average grain size. Tensile testing was conducted at quasi-static strain rate of 10^{-3} s^{-1} on flat specimens of 110 mm length and 6.25 mm width × 25 mm gauge length. Three specimens were tested for each condition, and average properties are reported. Hardness of the samples was measured on the surface of the specimens using Vickers hardness tester with a load and dwell time of 10 kgf and 10 s, respectively, and an average of six readings is reported. The x-ray diffraction (XRD) measurements were taken in the range of 40–100 (2theta) with a step size of 0.05 using a copper target. Dislocation density of the samples was determined from lattice strain calculated from XRD measurements by Hall–Williamson method. Ferrite content in the steel was measured using Fishers feritoscope FMP 30, and average of six readings is reported. Prior to measurement, instrument was calibrated with a standard specimen with ferrite content of 0.54% (605–564). The accuracy of measured ferrite content will be within ± 5%.

3. Results

3.1 Mechanical Properties

Hardness of the hot rolled (HR) samples showed a decreasing trend with increase in the rolling temperature as shown in Fig. 1. In the annealed condition, the steel showed a hardness of 260 VHN. The hardness of the hot rolled samples was in the range of 283–386 VHN. Maximum and minimum hardness of 386 and 283 VHN was observed in HR700 and HR1000 samples, respectively. It is interesting to note that all the hot rolled samples showed higher hardness than the annealed sample. The influence of rolling temperature on the tensile properties of the steel is shown in Fig. 2. The tensile properties in the annealed condition were ultimate tensile strength (UTS) of 678 MPa, yield strength (YS) of 352 MPa and ductility of 68%. An increase in ductility and decrease in strength were observed with the increase in the rolling temperature from 700 to 1000 °C. Maximum strength was observed in HR700 sample with UTS and YS of 971 MPa and 917 MPa, respectively, retaining good ductility of 25%. This variation in mechanical properties with the rolling temperature will be explained with the aid of dislocation and solid solution strengthening.

3.2 Microstructure

The microstructure of the annealed sample comprises of equiaxed austenitic grains with annealing twins and delta ferrite phase (pointed by arrows) as shown in Fig. 3. The amount of delta phase in the steel was 0.6%. Prior to measurement, the calibration was conducted using standard

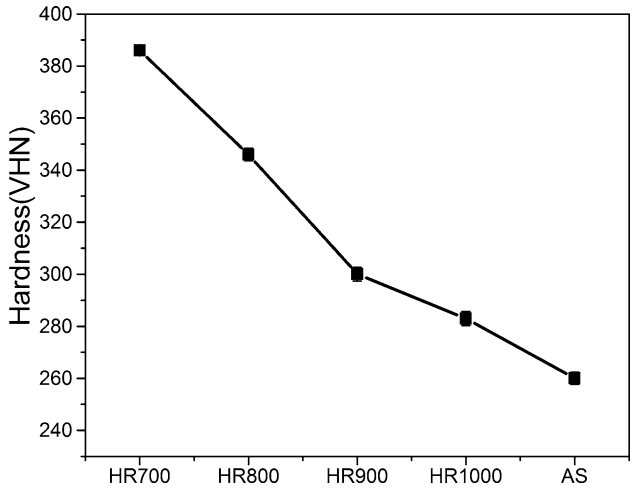

Fig. 1 Hardness of the steel in the annealed and hot rolled condition

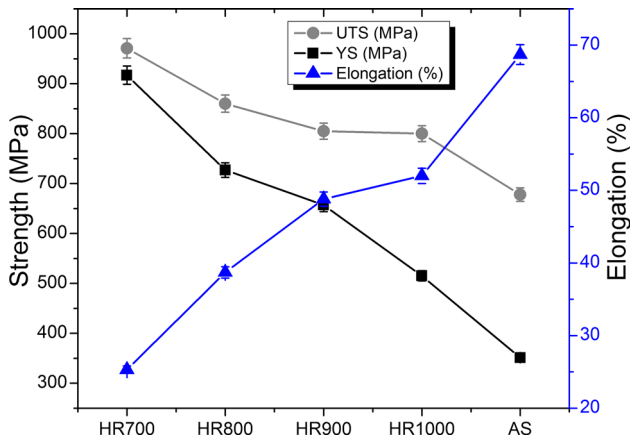

Fig. 2 Influence of hot rolling temperature on the tensile properties of the steel

(605–564). The average grain size including the annealing twins was measured to be 120 ± 15 μm. Figure 4 shows the optical micrographs of the samples hot rolled in the temperature range of 700–1000 °C. At rolling temperature of 700 °C, the original grains got elongated and grain boundaries were finely serrated (Fig. 4a). The length and width of the elongated grains were 213 ± 60 and 56 ± 22 μm, respectively. The twins present in initial microstructure are expected to transform to high angle grain boundaries (Ref 8). As the rolling temperature increased to 800 °C, the width of elongated grains increased to 70 ± 25 μm and the grain boundaries became more serrated as shown in Fig. 4(b). Dynamically recrystallized (DRx) grains with an average size of 19 ± 7 and 34 ± 13 μm were observed in the HR900 and HR1000 samples, respectively (Fig. 4c and d).

3.3 Dislocation Density

The two methods widely employed for determination of dislocation density are based on x-ray diffraction (XRD) (Ref 8) and transmission electron microscopy (TEM) (Ref 9). Dislocation density from TEM is quantified using Ham's interception method where the number of intersection points between the mesh and dislocations is determined to calculate the dislocation density (Ref 10). There are few difficulties with this method such as laborious specimen preparation and very small observation area (Ref 11), obtaining TEM images with good contrast covering maximum of number of dislocations, and determination of number of interceptions in the presence of dislocation cells/pileup/forests. Dislocation density measured from the XRD method is not very precise for the reasons mentioned elsewhere (Ref 12). Nevertheless, XRD is preferred over TEM for determination of dislocation indirectly from the lattice strain. The dislocation density was determined from the lattice strain using the following formula (Eq 1) (Ref 8),

$$\text{Dislocation density}(\rho) = 16.1\left(\frac{\varepsilon^2}{b^2}\right) \quad \text{(Eq 1)}$$

where b is the Burgers vector of dislocation ($b = a/\sqrt{2}$ for the fcc structure where a is the lattice parameter) and ε is the lattice strain. Hall–Williamson method was employed to the determine the lattice strain as the slope of the plot ($\beta\cos\theta$ vs $4\sin\theta$) where β is the integral breadth. The lattice strain and dislocation density of the hot rolled samples are given in Table 2. The dislocation density of the samples decreased with the rolling temperature with a maximum and minimum value of 1.4×10^{15} m^{-2} (HR700) and 2×10^{14} m^{-2} (HR1000), respectively. The dislocation density of the annealed sample was 4×10^{13} m^{-2}. This decreasing trend of dislocation density with rolling temperature is in agreement with the available literature (Ref 13-15).

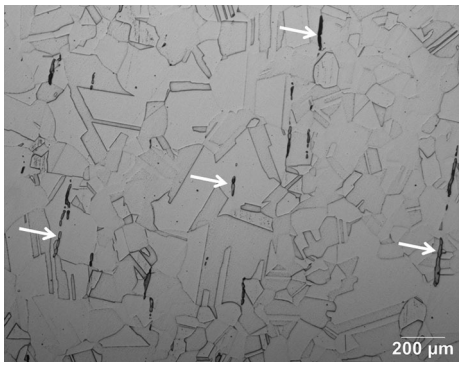

Fig. 3 Bright-field optical micrograph of the steel in the annealed condition (arrows pointing delta ferrite)

4. Discussion

4.1 Microstructural Evolution

The microstructural changes during hot rolling are function of the temperature, strain rate and strain (Ref 16, 17). Extensive work is done on the microstructural modeling during hot rolling of the steels, and empirical relations are proposed to determine the peak strain (ε_p), critical strain (ε_c) and grain size of dynamically recrystallized grains (Ref 16, 18-20). Critical strain (ε_c) indicates the nucleation of the dynamic recrystallization for a given temperature and strain rate (Ref 16). It is a function of initial grain size, strain rate and temperature which is determined using Eq 2 (Ref 19)

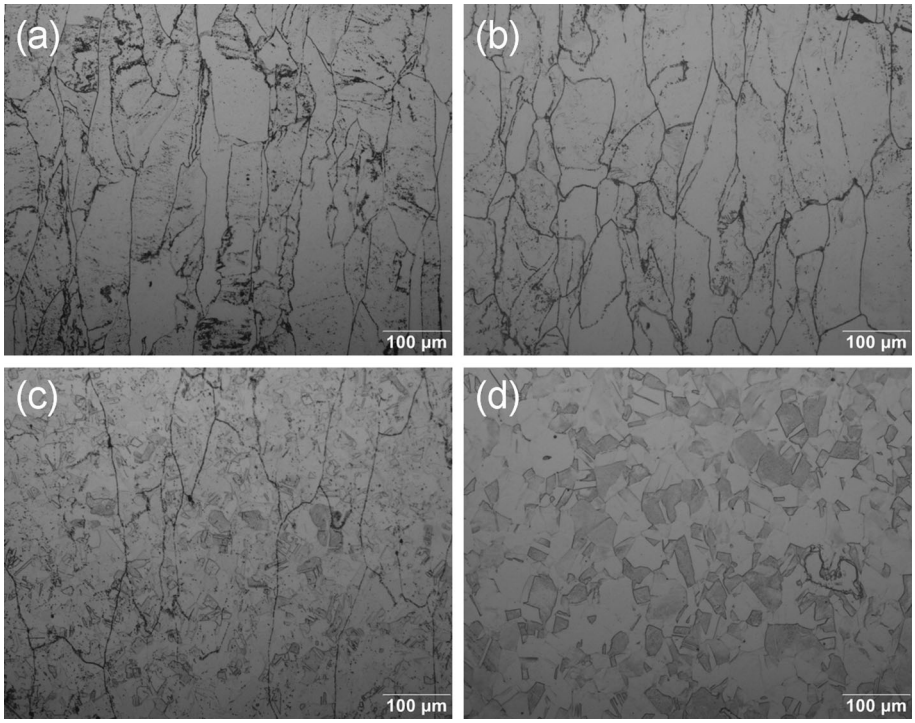

Fig. 4 Bright-field optical micrographs of the steel rolled at different temperatures: (a) 700 °C, (b) 800 °C, (c) 900 °C and (d) 1000 °C

$$\varepsilon_c = 2.1 \times 10^{-3} D_0^{0.5} Z^{0.09} \quad \text{(Eq 2)}$$

$$Z = \dot{\varepsilon} \times \exp(Q/\mathrm{RT}) \quad \text{(Eq 3)}$$

where D_o is the initial grain size (120 μm), $\dot{\varepsilon}$ is the strain rate (5.5 s^{-1}), Q is the activation energy (380 kJ mol^{-1}) (Ref 19), R is the universal gas constant (8.314 J mol^{-1} K^{-1}) and T is the temperature in K.

The dynamically recrystallized grain size of the hot rolled samples was determined using Eq 4 (Ref 19)

Table 2 Lattice strain and dislocation density of the steel calculated from XRD

Sample ID	Lattice strain	Dislocation density (m^{-2})
HR700	0.0024	1.4×10^{15}
HR800	0.0018	8.1×10^{14}
HR900	0.0012	3.6×10^{14}
HR1000	0.0009	2.0×10^{14}
Annealed	0.0004	4.0×10^{13}

Table 3 Critical strain and dynamically recrystallized grain size of the hot rolled samples

Temperature (K)	Zener–Hollomon parameter (Z)	Critical strain (ε_c)	D_{DRX} (μm)
973	1.3×10^{21}	1.83	…
1073	1.7×10^{19}	1.23	…
1173	4.5×10^{17}	0.89	10
1273	2.1×10^{16}	0.67	20

$$D_{DRx} = 139.5 - 7.3 \log Z \quad \text{(Eq 4)}$$

The critical strain and dynamically recrystallized grain size are summarized in Table 3. The total strain induced by hot rolling was 0.94 ($\varepsilon = 1.155 \ln ho/hf$ where ho is the initial thickness and hf is the final thickness). For the samples hot rolled at 900 and 1000 °C, the strain induced is higher than the critical strain and indicates the occurrence of dynamic recrystallization. The D_{DRx} determined using Eq 4 matched with the measured grain size in HR900 and HR1000 samples. The induced strain is less than critical strain for the samples rolled in the temperature range of 700–800 °C and resulted in the elongation of grains in the rolling direction without initiation of dynamic recrystallization (4a-4b). The development of the dynamic recrystallization (DRx) structure in the steel is summarized in Fig. 5 for a small part of microstructure. At 700–800 °C, the straight original grain boundaries got distorted and developed an irregular shape in the form of serrations and bulges as indicated by arrows (Fig. 5a and b). With an increase in the rolling temperature, the serrations separated from the prior grain boundaries and led to the formation of new recrystallized grains. In this manner, all the grain boundaries were occupied by DRx grains with average grain size of 19 ± 7 μm in HR900 as shown in Fig. 5(c). At 1000 °C, minor increase in recrystallized grain size was observed with average grain size of 34 ± 13 μm (Fig. 5d). To summarize, the microstructural changes in the hot rolled (700–1000 °C) samples are as follows: (i) formation of elongated grains in the rolling direction with serrated grain boundaries (700–800 °C) and (ii) nucleation of first DRx grains at the serrated grain boundaries followed by their growth to form fully recrystallized grains with annealing twins (900–1000 °C). In addition to these microstructural changes, the warm/hot-rolled

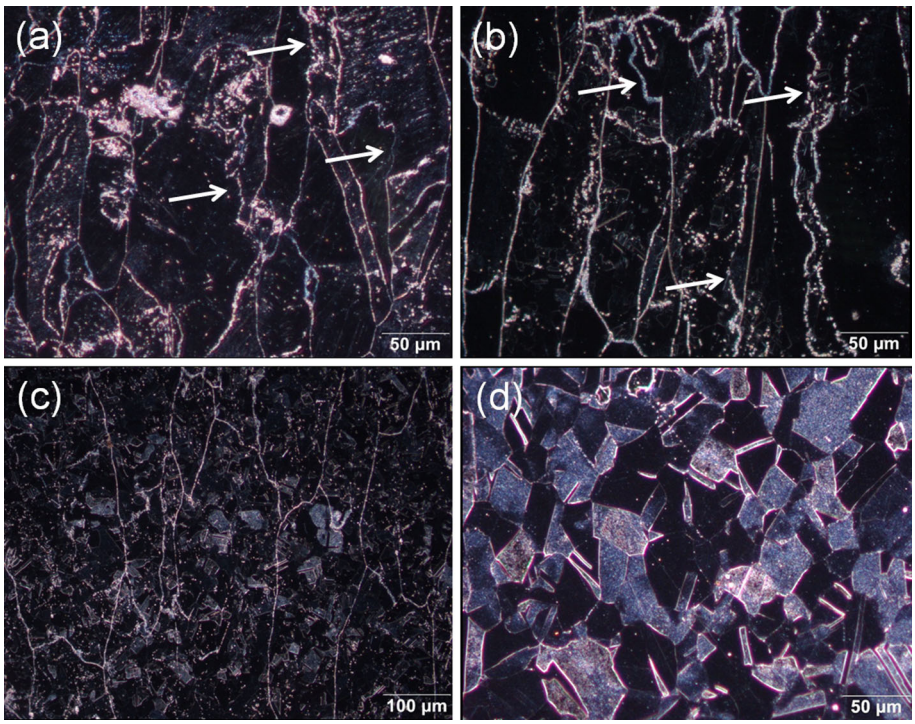

Fig. 5 Dark-field optical micrographs of the steels showing the microstructural changes during hot rolling: (a) rolled at 700 °C, (b) rolled at 800 °C, (c) rolled at 900 °C and (d) rolled at 1000 °C (arrows pointing the serrated grain boundaries)

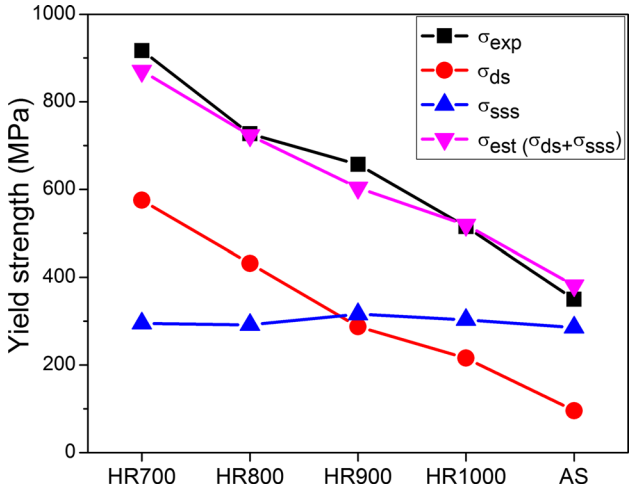

Fig. 6 Comparison of experimental and the estimated strength in the hot rolled and annealed condition: solid solution strengthening (σ_{sss}), dislocation strengthening (σ_{ds}), experimental strength (σ_{exp}) and estimated strength (σ_{est})

steels are characterized by the presence of high dislocation density (Ref 14, 21, 22).

4.2 Strengthening

The yield strength of the steel in the annealed condition was 352 MPa which is higher than classical ASS (SS304, SS316 and SS321) mainly due to the presence of nitrogen (Ref 23-25). Nitrogen acts as strong interstitial solid solution strengthener due to misfit between the interstitial element (*N*) and the octahedral voids which induces large lattice strain (Ref 24) and interaction/pinning of dislocations by the nitrogen atoms because of electrostatic attraction (Ref 26). The tensile properties of the hot rolled samples tested at ambient temperature are shown in Fig. 2. Tensile properties varied with the rolling temperature, and reduction in the rolling temperature resulted in significant strengthening of the steel. An increase of 160% in the yield strength was observed in HR700 sample compared to the annealed condition. The strengthening achieved by hot rolling was accompanied by degradation in the tensile ductility. The ductility has gradually decreased from 52% at 1000 °C to about 25% at 700 °C. The changes in tensile properties with rolling temperature correlate well with the microstructure (Fig. 4 and 5) and dislocation density (Table 2). The lower ductility at 700 °C may be attributed to high dislocation density and deformed grains which restrict the strain hardening and degrade the ductility.

The yield strength of the austenitic stainless steel depends on the contribution from solid solution, dislocation density and grain size (Ref 14, 27, 28). The strength due to solid solution strengthening and grain size in ASS can be estimated using empirical formulae based on the chemical composition and grain size (Ref 27-29). One such empirical relation (Eq 5) was employed to estimate the yield strength due to solid solution strengthening and grain size (Ref 27).

$$\sigma_{sss}(\text{MPa}) = 68 + 493\text{N} + 354\text{C} + 14\text{Mo} + 3.7\text{Cr} + 20\text{Si} + 0.22\text{D}^{-\left(\frac{1}{2}\right)} + 2.5\delta \quad \text{Eq 5}$$

where D is the grain size and δ is the area fraction of delta ferrite phase. The coefficients for the elements are given in (MPa/wt.%), amount of alloying elements in wt.%, for the ferrite content in (MPa/area fraction %) and for the grain size in (MPa $m^{0.5}$)

Another significant source of strengthening in the hot rolled metals and alloys is dislocations. The contribution of dislocations to the yield strength can be estimated using Eq 6 (Ref 24).

$$\sigma_{ds}(\text{MPa}) = M\alpha\text{Gb}\sqrt{\rho} \quad \text{(Eq 6)}$$

where M 3.06 is the Taylor factor, α-0.26 is the geometrical factor (Ref 12), G-75,000 MPa is the shear modulus (Ref 30), b-0.253 nm is the Burgers vector and ρ is the dislocation density in m^{-2}. The estimated yield strength is the summation of the contribution from the solid solution and dislocation strengthening as shown in Eq 7

$$\sigma_{est} = \sigma_{sss} + \sigma_{ds} \quad \text{(Eq 7)}$$

Figure 6 shows the contribution from solid solution strengthening (σ_{sss}), dislocation strengthening (σ_{ds}), experimental yield strength (σ_{exp}) and estimated yield strength (σ_{est}) for the steel in the hot rolled condition. The contribution from the dislocations showed a decreasing trend with an increase in the rolling temperature, and it is lowest for the annealed sample. On the other hand, the contribution from the solid solution strengthening was in the range of 285–316 MPa. The estimated yield strength closely matches with the experimental values for all the samples. To summarize, the strengthening by multi-pass hot rolling is mainly influenced by change in the grain size and dislocation density. At higher rolling temperature (900–1000 °C), high ductility and moderate strength were obtained due to lower dislocation density and fully recrystallized grains. On the other hand, at lower rolling temperature (700–800 °C) high strength achieved was attributed to high dislocation density.

5. Conclusions

The influence of multi-pass hot rolling in the temperature range of 700–1000 °C on the microstructure and mechanical properties of nitrogen alloyed austenitic stainless steel was studied, and the following conclusions are drawn: Hot rolling in the temperature range of 700–800 °C resulted in the formation of elongated grains coupled with high dislocation density. At higher rolling temperature (900–1000 °C), fine fully recrystallized grains were observed and dislocation density was in the range of 2.0–3.6 × 10^{14} m^{-2}. Hot rolled samples showed higher tensile strength than annealed samples. The yield strength of 917 MPa and ductility of 25% was achieved by rolling at 700 °C. The yield strength of the hot rolled steel could be evaluated as the summation of solid solution strengthening, grain boundary strengthening and dislocation strengthening.

Acknowledgment

The authors would like to thank their colleagues at Material Characterization Division (VSSC) for their support in mechanical testing, metallography and XRD measurement of the samples. The authors would also like to thank Director, Vikram Sarabhai Space Centre, Thiruvananthapuram, for his kind permission to publish this work.

References

1. Y. Fu, X. Wu, E.H. Han, W. Ke, K. Yang, and Z. Jiang, Effects of Nitrogen on the Passivation of Nickel-Free High Nitrogen and Manganese Stainless Steels in Acidic Chloride Solutions, *Electrochim. Acta*, 2009, **54**, p 4005–4014. https://doi.org/10.1016/j.electacta.2009.02.024
2. H. Baba, T. Kodama, and Y. Katada, Role of Nitrogen on the Corrosion Behavior of Austenitic Stainless Steels, *Corros. Sci.*, 2002, **44**, p 2393–2407. https://doi.org/10.1016/S0010-938X(02)00040-9
3. M. Pozuelo, J.E. Wittig, J.A. Jiménez, and G. Frommeyer, Enhanced Mechanical Properties of a Novel High-Nitrogen Cr-Mn-Ni-Si Austenitic Stainless Steel via TWIP/TRIP Effects, *Metall. Mater. Trans. A Phys. Metall. Mater. Sci.*, 2009, **40**, p 1826–1834. https://doi.org/10.1007/s11661-009-9863-8
4. H. Li, Z. Jiang, Z. Zhang, and Y. Yang, Effect of Grain Size on Mechanical Properties of Nickel-Free High Nitrogen Austenitic Stainless Steel, *J. Iron. Steel Res. Int.*, 2009, **16**, p 58–61. https://doi.org/10.1016/S1006-706X(09)60011-X
5. S. Fréchard, A. Redjaïmia, E. Lach, and A. Lichtenberger, Mechanical Behaviour of Nitrogen-Alloyed Austenitic Stainless Steel Hardened by Warm Rolling, *Mater. Sci. Eng. A*, 2006, **415**, p 219–224. https://doi.org/10.1016/j.msea.2005.09.070
6. A. Di Schino and J.M. Kenny, Grain Refinement Strengthening of a Micro-Crystalline High Nitrogen Austenitic Stainless Steel, *Mater. Lett.*, 2003, **57**, p 1830–1834. https://doi.org/10.1016/S0167-577X(02)01076-5
7. D.W. Kim, Influence of Nitrogen-Induced Grain Refinement on Mechanical Properties of Nitrogen Alloyed Type 316LN Stainless Steel, *J. Nucl. Mater.*, 2012, **420**, p 473–478. https://doi.org/10.1016/j.jnucmat.2011.11.001
8. G.K.S.R.E. Williamson, Dislocation Densities in Some Annealed and Cold-Worked Metals from Measurements on the X-ray Debye-Scherrer Spectrum, *Philos. Mag.*, 1956, **1**, p 34–46. https://doi.org/10.1080/14786435608238074
9. R.K. Ham, The Determination of Dislocation Densities in Thin Films, *Philos. Mag.*, 1961, **6**, p 1183–1184
10. Y. Miyajima, M. Mitsuhara, S. Hata, H. Nakashima, and N. Tsuji, Quantification of Internal Dislocation Density Using Scanning Transmission Electron Microscopy in Ultrafine Grained Pure Aluminium Fabricated by Severe Plastic Deformation, *Mater. Sci. Eng. A*, 2010, **528**, p 776–779. https://doi.org/10.1016/j.msea.2010.09.058
11. T.G. Sousa, S.B. Diniz, A.L. Pinto, and L.P. Brandao, Dislocation Density by X-ray Diffraction in α Brass Deformed by Rolling and ECAE, *Mater. Res.*, 2015, **18**, p 246–249. https://doi.org/10.1590/1516-1439.369214
12. G. Dini, R. Ueji, A. Najafizadeh, and S.M. Monir-Vaghefi, Flow Stress Analysis of TWIP Steel via the XRD Measurement of Dislocation Density, *Mater. Sci. Eng. A*, 2010, **527**, p 2759–2763. https://doi.org/10.1016/j.msea.2010.01.033
13. S.C. Krishna, G.S. Rao, A.K. Jha, B. Pant, and P.V. Venkitakrishnan, Strengthening in High Strength Cu-Cr-Zr-Ti Alloy Plates Produced by Hot Rolling, *Mater. Sci. Eng. A*, 2016, **674**, p 164–170
14. Z. Yanushkevich, A. Mogucheva, M. Tikhonova, A. Belyakov, and R. Kaibyshev, Structural Strengthening of an Austenitic Stainless Steel Subjected to Warm-to-Hot Working, *Mater. Charact.*, 2011, **62**, p 432–437. https://doi.org/10.1016/j.matchar.2011.02.005
15. F. Yin, T. Hanamura, O. Umezawa, and K. Nagai, Phosphorus-Induced Dislocation Structure Variation in the Warm-Rolled Ultrafine-Grained Low-Carbon Steels, *Mater. Sci. Eng. A*, 2003, **354**, p 31–39. https://doi.org/10.1016/S0921-5093(02)00766-9
16. C.M. Sellars, Modelling Microstructural Development During Hot Rolling, *Mater. Sci. Technol.*, 1990, **6**, p 1072–1081. https://doi.org/10.1179/026708390790189966
17. C.M. Sellars and J.A. Whiteman, Recrystallization and Grain Growth in Hot Rolling, *Met Sci*, 1978, **13**, p 187–194. https://doi.org/10.1179/msc.1979.13.3-4.187
18. M. Jafari and A. Najafizadeh, Correlation Between Zener-Hollomon Parameter And Necklace DRX During Hot Deformation of 316 Stainless Steel, *Mater. Sci. Eng. A*, 2009, **501**, p 16–25. https://doi.org/10.1016/j.msea.2008.09.073
19. S. Cho and Y. Yoo, Hot rolling simulations of austenitic stainless steel, *J. Mater. Sci.*, 2001, **36**, p 4267–4272
20. Z. Wang, W. Fu, S. Sun, H. Li, Z. Lv, and D. Zhao, Mechanical Behavior and Microstructural Change of a High Nitrogen CrMn Austenitic Stainless Steel During Hot Deformation, *Metall. Mater. Trans. A*, 2010, **41**, p 1025–1032. https://doi.org/10.1007/s11661-009-0153-2
21. S.C. Krishna, N.K. Gangwar, A.K. Jha, B. Pant, and P.V. Venkitakrishnan, On the Direct Aging of Iron Based Superalloy Hot Rolled Plates, *Mater. Sci. Eng. A*, 2015, **648**, p 274–279. https://doi.org/10.1016/j.msea.2015.09.073
22. K. Nakashima, M. Suzuki, Y. Futamura, T. Tsuchiyama, and S. Takaki, Limit of Dislocation Density and Dislocation Strengthening in Iron, *Mater. Sci. Forum*, 2006, **503–504**, p 627–632. https://doi.org/10.4028/www.scientific.net/MSF.503-504.627
23. Y. Murata, S. Ohashi, and Y. Uematsu, Recent Trends in the Production and Use of High Strength Stainless Steels, *ISIJ Int.*, 1993, **33**, p 711–720
24. G. Balachandran, M.L. Bhatia, N.B. Ballal, and P.K. Rao, Processing Nickel Free High Nitrogen Austenitic Stainless Steels Through Conventional Electroslag Remelting Process, *ISIJ Int.*, 2000, **40**, p 478–483. https://doi.org/10.2355/isijinternational.40.478
25. V.G. Gavriljuk, Nitrogen in Iron and Steel, *ISIJ Int.*, 1996, **36**, p 738–745. https://doi.org/10.2355/isijinternational.36.738
26. K.H. Lo, C.H. Shek, and J.K.L. Lai, Recent Developments in Stainless Steels, *Mater. Sci. Eng. R Rep.*, 2009, **65**, p 39–104. https://doi.org/10.1016/j.mser.2009.03.001
27. H. Sieurin, J. Zander, and R. Sandström, Modelling Solid Solution Hardening in Stainless Steels, *Mater. Sci. Eng. A*, 2006, **415**, p 66–71. https://doi.org/10.1016/j.msea.2005.09.031
28. G. Balachandran, M.L. Bhatia, N.B. Ballal, and P.K. Rao, Some Theoretical Aspects on Designing Nickel Free High Nitrogen Austenitic Stainless Steels, *ISIJ Int.*, 2001, **41**, p 1018–1027. https://doi.org/10.2355/isijinternational.41.1018
29. J. Eliasson and R. Sandström, Proof Strength Values for Austenitic Stainless Steels at Elevated Temperatures, *Steel Res. Int.*, 2000, **71**, p 249–254
30. L. Vitos, P.A. Korzhavyi, and B. Johansson, Elastic Property Maps of Austenitic Stainless Steels, *Phys. Rev. Lett.*, 2002, **88**, p 155501